# Angular spectrum of light transmitted through turbid media: theory and experiment

Alexander A. Kokhanovsky, Reiner Weichert, Michael Heuer, and Wolfgang Witt

Measurements of the angular spectrum of light transmitted through turbid slabs with monodispersions of polystyrene spheres have been performed. The results obtained are compared with theoretical calculations, based on the small-angle approximation of the radiative transfer theory. The experimental data and the theoretical results coincide with a high accuracy, which allows us to develop the laser diffraction spectroscopy of optically thick light-scattering layers. © 2001 Optical Society of America

*OCIS codes:* 010.1290, 010.1110, 010.3310, 010.4450, 120.5820, 290.4210.

## 1. Introduction

The analysis of the Fraunhofer diffraction patterns of different light-scattering media is a standard tool in the field of particulate media characterization.[1] Both the size[2] and the shape[3] of particles can be retrieved from angular dependencies of the scattered light at small observation angles. For instance, it follows for polydispersions of large spherical particles ($ka \gg 1$, $2|m-1|ka \gg 1$, $k = 2\pi/\lambda$, where $\lambda$ is the wavelength, $m$ is the relative refractive index, and $a$ is the radius of particles),[2]

$$I(\theta) = C\theta^{-2}\int_0^\infty a^2 f(a) J_1{}^2(ka\theta)\mathrm{d}a, \tag{1}$$

where $C = \text{const}$, $f(a)$ is the particle size distribution, $I(\theta)$ is the measured scattered intensity, $\theta$ is the scattering angle, and $J_1(k\theta a)$ is the Bessel function. There are many methods to retrieve the particle size distribution $f(a)$ from Eq. (1).[2] They have already been incorporated into the software of modern particle sizers.[1,4–6]

Equation (1) can be applied only in the case of thin turbid layers, when the multiple light scattering is negligible. However, there is a need for information on particle size distributions in dense media with strong multiple light scattering. This is because some media (e.g., in solid state) cannot be diluted or are not under control (e.g., various aerosols and clouds in the sky). The inverse problem for multiply scattering media was formulated and solved in Refs. 7–11.

Our task in this paper is the experimental study of the influence of the multiple light scattering on Fraunhofer diffraction patterns of polysterene spherical particles. Experiments were carried out with the standard commercially available Sympatec Particle Sizer.[5] Particles were almost monodispersed and characterized by mode radii near 5 and 50 μm. The results of experiments were compared with theoretical solutions, obtained in Ref. 12.

## 2. Experiment

The experimental setup is presented in Fig. 1. A He–Ne laser beam with the wavelength $\lambda = 0.6328$ μm passes through a beam expander and a sample with monodispersions of polystyrene spheres. The diffraction pattern is measured with the help of the detector with 31 semicircular elements of a different width.[5] Polystyrene spheres with certified mean diameters $d_0$ equal to $100 \pm 2.0$ μm and $9.685 \pm 0.064$ μm have been used in the experiment. The coefficient of variation of the particle size distribution was equal to 0.042 for large particles and 0.014 for smaller ones. Particles were composed of polystyrene DVB (divinylbenzene, 4–8%) and had the spe-

When this research was performed, A. A. Kokhanovsky (alex@zege.bas.net.by) was with the Department of Chemical Engineering and Chemical Technology, Imperial College of Science, Technology and Medicine, London SW7 32BY, UK, and with the Institute of Physics, 70 Skarina Avenue, Minsk, Belarus. He is now with the Institute of Environmental Physics, University of Bremen, Bremen D-28334, Germany. R. Weichert is with the Institute of Particle Technology, Clausthal Technical University, Leibnizstrasse 19, D-38658 Clausthal-Zellerfeld, Germany. M. Heuer and W. Witt are with Sympatec GmbH, D-38644 Goslar, Germany.

Received 26 June 2000; revised manuscript received 2 January 2001.

0003-6935/01/162595-06$15.00/0

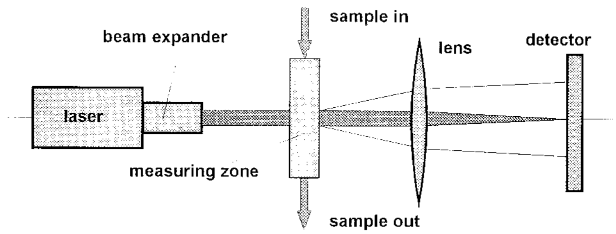


Fig. 1. Experimental setup.

cific gravity 1.05 g/ml. The refractive index of particles at the wavelength 0.59 μm was equal to 1.59.

The results of the experiment are presented in Figs. 2 and 3 for different optical thicknesses $\tau$ and sizes of particles. Diameters of particles were much larger than the wavelength of the incident light. Note that it follows in a good approximation for the

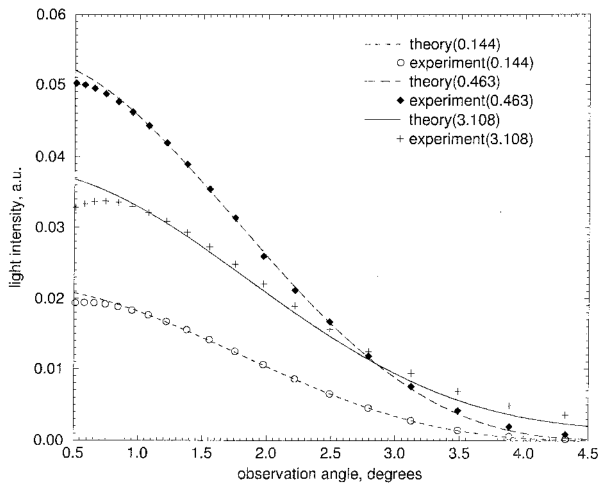


Fig. 2. Angular dependence of the light transmitted through a sample with polystyrene spherical particles according to the experiment and the theory at the optical thickness equal to 0.144, 0.463, and 3.108. The diameter of spheres is equal to 9.685 μm.

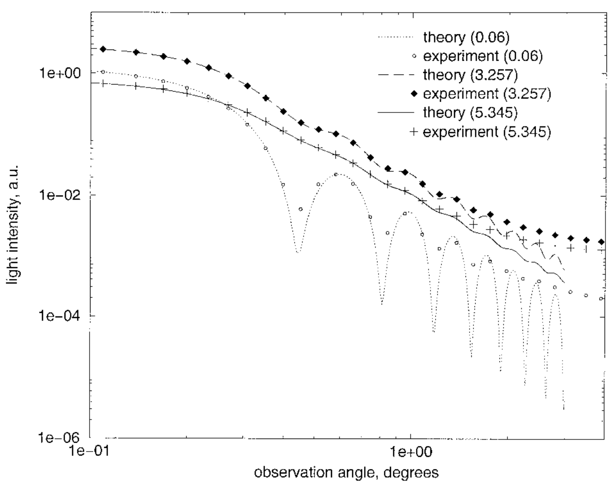


Fig. 3. Same as Fig. 2 but with diameter of spheres of 100 μm and optical thickness equal to 0.06, 3.257, and 5.345.

extinction efficiency factor $Q_{\text{ext}} = 2$ in this case. Thus the optical thickness is approximately given by[13] $\tau = 3Lc/d_{ef}$, where where $d_{ef}$ is the Sauter diameter of particles, $L$ is the geometrical thickness of a sample, and $c$ is the volumetric concentration of particles in the suspension. It follows for the value of $c$ that

$$c = d_{ef}\tau/3L.$$

One can see that the value of $c$ is simply expressed by the optical thickness of the medium $\tau$. The value of $\tau$ was measured independently during the experiment. The geometrical thickness $L$ was equal to 20 mm and $d_{ef} \approx d_0$, owing to the high monodispersity of particles in a sample.

The experiment (symbols) shows that the increase in the concentration of particles leads to higher values of the transmitted intensity in the region of small values of $\tau$. However, the transmitted intensity reduces with further growth of the optical thickness.

Indeed, the intensity of the transmitted diffused light $I_d$ is equal to zero if there are no particles in a cuvette. It grows with the optical thickness initially. However, it is equal to zero for semi-infinite media. Thus it should be a maximum in the dependencies $I_d(\tau)$ at some value of $\tau$. This is in correspondence with our experimental results. It should be noted that oscillations in Fig. 3 confirm the high monodispersity of particles in a sample.

Another interesting feature is related to the broadening of the diffraction pike due to the multiple light-scattering phenomenon. The larger the optical thickness $\tau$, the larger the half-width of the angular spectrum of the transmitted light. It should be noted that the half-widths of the small-angle peaks of the scattered light also increase with the decrease of particle size [see Eq. (1)]. Thus the presence of multiple light scattering could lead to underestimation of particle size in the standard inversion procedures, which do not account for multiple light scattering.

Figures 2 and 3 differ owing to the absence of minima in Fig. 2 for low concentrations of particles. This is due to the limitation of observation angles by 4° in the experiment. The first minimum should appear at the scattering angle

$$\theta_d = \frac{3.83 \times 180}{\pi x}$$

degrees according to the Fraunhofer theory.[14] Here $x = 2\pi a/\lambda$ is the size parameter. The value of $\theta_d$ is approximately equal to 0.4° at $a = 50$ μm. But it is ~4° at $a = 5$ μm, which is almost outside the measured angular range.

It should be noted that multiple light scattering reduces oscillations and makes diffraction patterns more smooth. The same effect could be due to the polydispersity of particles in a turbid medium.

## 3. Theory

The diffused transmitted intensity can be found from the solution of the radiative transfer equation.[12,13,15–17] This equation is written in the following form in the case of the normal illumination of a scattering plane–parallel layer with randomly oriented particles by a plane wave,

$$\cos\vartheta\,\frac{dI(\tau,\vartheta)}{d\tau}=-I(\tau,\vartheta)+\frac{\omega_0}{2}\int_0^{\pi}I(\tau,\vartheta')p(\vartheta,\vartheta')\times\sin\vartheta' d\vartheta', \tag{2}$$

where $\vartheta$ is the observation angle; $\omega_0=\sigma_{sca}/\sigma_{ext}$ is the single-scattering albedo; $\sigma_{sca}$ and $\sigma_{ext}$ are scattering and extinction coefficients; $\tau=\sigma_{ext}L$ is the optical thickness; $L$ is the geometrical thickness of a layer; $p(\vartheta,\vartheta')=\frac{1}{2}\int_0^{2\pi}p(\theta)d\varphi$ is the phase function, averaged on the relative azimuth $\varphi$; $I$ is the light intensity; and $\theta=\arccos(\cos\vartheta\cos\vartheta'+\sin\vartheta\sin\vartheta'\cos\varphi)$ is the scattering angle. It should be noted that Eq. (2) does not account for the spatial width and the angular spread of the incident beam. Thus it can be used only if the beam cross section is sufficiently large, which is the case for our experiment (see Fig. 1).

Our primary task here is to study the influence of multiple light scattering on Fraunhofer diffraction patterns in optically dense disperse layers. Thus we consider the behavior of the function $I(\tau,\vartheta)$ at small values $\vartheta$ and assume that

$$\cos\vartheta\,\frac{dI(\tau,\vartheta)}{d\tau}\approx\frac{dI(\tau,\vartheta)}{d\tau}.$$

It follows from Eq. (2) in this case that

$$\frac{dI(\tau,\vartheta)}{d\tau}=-I(\tau,\vartheta)+\frac{\omega_0}{2}\int_0^{\pi}I(\tau,\vartheta')p(\vartheta,\vartheta')\sin\vartheta' d\vartheta'. \tag{3}$$

The integral in Eq. (3) accounts for the multiple scattering of photons from all scattering directions to the direction specified by the observation angle $\vartheta$. It should be noted that the function $I(\tau,\vartheta')$ is characterized by a rather sharp peak at $\vartheta'\approx 0$ (see, e.g., the results of our experiment in Figs. 2 and 3). The same is true for the phase function $p(\theta)$, which is highly peaked in the forward-scattering direction for particles large compared with the wavelength of the incident radiation. This allows us to change the limit of integration in the integral term of Eq. (3) from $\pi$ to $\infty$ and obtain the following approximate transport equation,

$$\frac{dI(\tau,\vartheta)}{d\tau}=-I(\tau,\vartheta)+\frac{\omega_0}{2}\int_0^{\infty}I(\tau,\vartheta')p(\vartheta,\vartheta')\vartheta' d\vartheta', \tag{4}$$

where we accounted for the fact that $\sin\vartheta'\approx\vartheta'$ as $\vartheta'\to 0$ and the phase function $p(\theta)$ is normalized by the following condition:

$$\frac{1}{2}\int_0^{\infty}p(\theta)\theta d\theta=1. \tag{5}$$

One should expect that approximation (4) provides a high accuracy at small values of $\vartheta$, which are of interest in this paper. Equation (4) can be exactly solved with several different techniques. For instance, one can perform the Fourier transform of this equation and obtain[12]

$$I(\tau,\vartheta)=\frac{I_0}{2\pi}\int_0^{\infty}\exp\{-\tau[1-\omega_0P(\sigma)]\}J_0(\sigma\vartheta)\sigma d\sigma, \tag{6}$$

assuming that the intensity of the incident wave is

$$I(0,\vartheta)=I_0\delta(\vartheta), \tag{7}$$

where

$$\delta(\vartheta)=\frac{1}{2\pi}\int_0^{\infty}J_0(\sigma\vartheta)\sigma d\sigma \tag{8}$$

is the delta function and $I_0$ is the constant. Here $J_0(\sigma\vartheta)$ is the Bessel function. The function

$$P(\sigma)=\frac{1}{2}\int_0^{\infty}p(\theta)J_0(\sigma\theta)\theta d\theta \tag{9}$$

in Eq. (6) is the Fourier–Bessel transform of the phase function $p(\theta)$. It is called the space-frequency decay function. One can see that $P(\sigma=0)=1$ as a result of the normalization condition (5). It is easy to verify solution (6) by means of substituting it into Eq. (4).

Thus Eq. (6) allows us to investigate diffraction patterns of multiply scattering layers by simple means. Let us subtract the coherent component of a light field $I_0\delta(\vartheta)\exp(-\tau)$ [see Eq. (8)] from the general solution (6). Then it follows for the diffused transmitted light $I_d(\tau,\vartheta)$ that

$$I_d(\tau,\vartheta)=\frac{I_0}{2\pi}\exp(-\tau)\int_0^{\infty}\{\exp[\omega_0P(\sigma)\tau]-1\}\times J_0(\sigma\vartheta)\sigma d\sigma. \tag{10}$$

This equation can be simplified in the case of thin layers. It follows from Eq. (10) as $\tau\to 0$ that

$$I_d(\tau,\vartheta)=(I_0/4\pi)\omega_0\tau p(\vartheta), \tag{11}$$

where [see Eq. (9)]

$$p(\vartheta)=2\int_0^{\infty}P(\sigma)J_0(\sigma\vartheta)\sigma d\sigma. \tag{12}$$

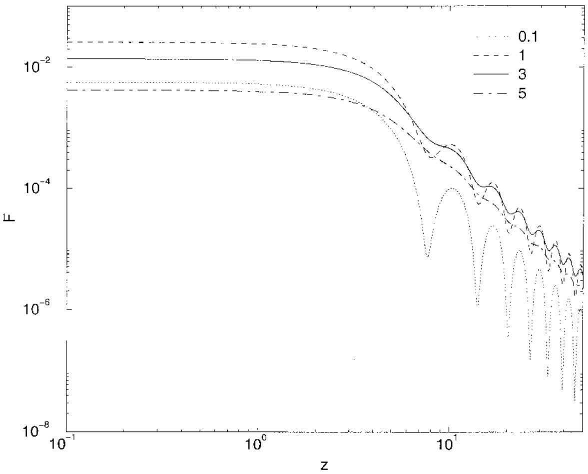


Fig. 4. Dependence $F(z)$ at different values of optical thickness equal to 0.1, 1, 3, and 5.

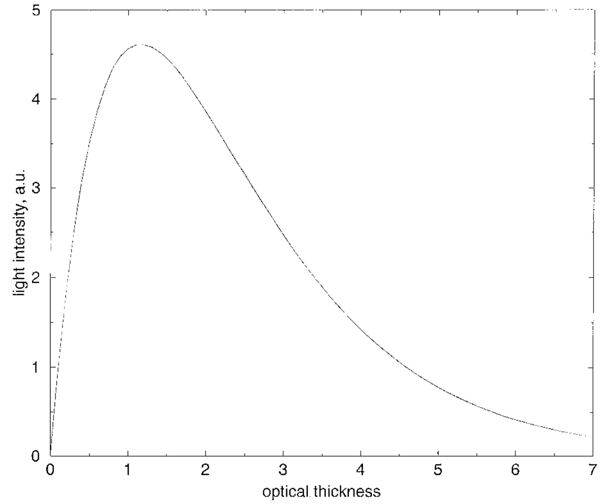


Fig. 5. Dependence of transmitted diffused light intensity [see Eqs. (15) and (16)] on optical thickness at $z = 1.5$.

Thus the small-angle diffused intensity is determined by the angular distribution of singly scattered light as it should be for small values of the optical thickness.

Equation (10) allows us to study the dependence of diffraction patterns on the optical thickness and concentration of particles. To do so, we should know the function $P(\sigma)$ in Eq. (10). That function differs for particles of different shapes and internal structures. For instance, it follows in the framework of the Fraunhofer approximation for monodispersed spherical particles[16] that

$$\omega_0 = \frac{1}{2}, \qquad p(\theta) = \frac{4J_1^{\,2}(\theta x)}{\theta^2}. \tag{13}$$

From Eqs. (9) and (13) one can obtain

$$P(\sigma) = \frac{2}{\pi}\left\{\arccos\left(\frac{\sigma}{2x}\right) - \frac{\sigma}{2x}\left[1 - \left(\frac{\sigma}{2x}\right)^2\right]^{1/2}\right\} u\left(\frac{\sigma}{2x}\right), \tag{14}$$

where $u(\sigma/2x) = 1$ at $\sigma \leq 2x$ and $u(\sigma/2x) = 0$ at $\sigma > 2x$. Thus the diffused intensity $I_d(\tau, \vartheta)$ can be presented in the following form [see Eq. (10)]:

$$I_d(\tau, \vartheta) = DF(\tau, \alpha), \tag{15}$$

where $D = 2x^2 I_0/\pi$ is the constant, which does not depend on the concentration of particles, and the function

$$F(\tau, z) = \exp(-\tau) \int_0^1 \left(\exp\left\{\frac{\tau}{\pi}\left[\arccos(y) - y(1 - y^2)^{1/2}\right]\right\} - 1\right) J_0(yz) y \mathrm{d}y \tag{16}$$

depends only on the optical thickness $\tau$ and the parameter $z = 2\vartheta x$. The function $F(z)$ at $\tau = 0.1$, 1, 3, and 5 is presented in Fig. 4. One can see that the intensity of the diffused transmitted light increases with the optical thickness, reaches the maximal values, and starts to decrease. The amplitude of oscillations decreases with the optical thickness $\tau$. However, the half-width of the small-angle peak increases with the optical thickness. All these features are consistent with the experimental data presented in Figs. 2 and 3.

The dependence of light intensity [Eq. (15)] on the optical thickness at $z = 1.5$ is presented in Fig. 5. One can see that the maximum of the intensity at the fixed angle occurs at $\tau \approx 1$ in this case. It should be noted that the function $I_d(\tau, \vartheta)$ in Fig. 5 was normalized to 1 at $\tau = 0.1$.

## 4. Comparisons of Computed and Experimental Results

Let us compare results of calculations with the experimental data obtained. To this end results of calculations with Eqs. (15) and (16) were matched to the experimental data at $\theta = 1°$ for smaller particles (see Fig. 2) and at $\theta = 0.1°$ for larger particles (see Fig. 3). The agreement between theory and experiment is excellent for all optical thicknesses except tails of the angular distributions of transmitted light (see, in particular, Fig. 3). Thus simple Eq. (16) can be indeed used for solution of both the inverse and the direct problems of light-scattering media optics.

The poor agreement of the theory and experiment at $\vartheta > 2°$ in Fig. 3 is due to the fact that multiple scattering of light refracted and reflected by particles[15–17] becomes important in this case. This is not accounted for in Eq. (16), where the geometrical optics component of the scattered light is simply neglected. Accounting for the geometrical optics scattering becomes important for larger particles at smaller scattering angles than it is for smaller particles (see Figs. 2 and 3). This is due to smaller half-widths of Fraunhofer diffraction patterns for larger scatterers.

Accounting for the geometrical optics scattering is

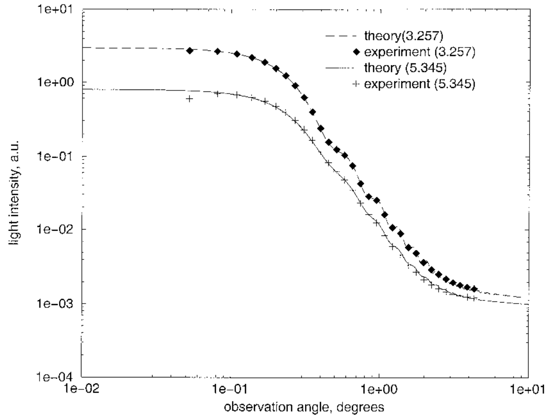


Fig. 6. Angular dependence of light intensity according to the experiment and the theory for samples with polystyrene spheres of 100-$\mu$m diameter with accounting for the geometrical optical scattering at optical thickness equal to 3.257 and 5.345.

rather simple. Indeed, neglecting the interference between diffracted, reflected, and refracted beams, one obtains[16]

$$p(\theta) = \frac{\sigma_{sca}{}^{d} p^{d}(\theta) + \sigma_{sca}{}^{g} p^{g}(\theta)}{\sigma_{sca}{}^{d} + \sigma_{sca}{}^{g}},$$

where $\sigma_{sca}{}^{d}$ and $\sigma_{sca}{}^{g}$ are parts of the total scattering coefficient $\sigma_{sca} = \sigma_{sca}{}^{d} + \sigma_{sca}{}^{g}$, related to diffraction and geometrical optics scattering processes, respectively.

It follows that $\sigma_{sca}{}^{d} = \sigma_{sca}{}^{g}$ for large transparent particles[18,19] and that

$$p(\theta) = \frac{p^{d}(\theta) + p^{g}(\theta)}{2}. \qquad (17)$$

The function $p^{d}(\theta)$ is described by Eq. (13), and the function $p^{g}(\theta)$ represents the geometrical optics contribution to the phase function $p(\theta)$. Note that functions $p^{d}(\theta)$, $p^{g}(\theta)$, and $p(\theta)$ are normalized according to Eq. (5).

Calculations performed in the framework of the geometrical optics approximation[15–17] show that the function $p^{g}(\theta)$ can be approximated by the following simple formula:

$$p^{g}(\theta) = 4\beta \exp(-\beta\theta^{2}), \qquad (18)$$

where the value of $\beta$ depends only on the refractive index of transparent particles and not on their size. The multiplier $4\beta$ in Eq. (18) is due to the normalization condition (5).

For the Fourier–Bessel transform (9) of the phase function (17) it follows that

$$P(\sigma) = \frac{P^{d}(\sigma) + P^{g}(\sigma)}{2}, \qquad (19)$$

where the value of $P^{d}(\sigma)$ can be found from Eq. (14) and [see Eqs. (9) and (18)],

$$P^{g}(\sigma) = \exp(-\sigma^{2}/4\beta). \qquad (20)$$

Results of the comparison of the calculated diffused transmitted intensity [see Eqs. (10) and (19)] with experimental data for monodipersed spheres with a 100-$\mu$m diameter are presented in Fig. 6. One can see that accounting for the geometrical optics scattering [see Eqs. (19) and (20)] indeed provides higher accuracy at larger values of $\vartheta$. Note that the value of $\beta = 5$ in Eq. (20) was obtained by fitting of experimental and theoretical results.

It should be noted that Eq. (10) is also valid for randomly oriented nonspherical particles and for polydispersed media. However, these media are characterized by different spectra $P(\sigma)$ as compared with the simple case of monodispersed spheres. This results in different angular spectra $I_{d}(\tau, \vartheta)$ of the diffused light. For instance, for disperse media with polydispersions of spherical particles it follows that[16]

$$\langle P(\sigma)\rangle = \frac{\int_{0}^{\infty} a^{2} f(a) P(\sigma) \mathrm{d}a}{\int_{0}^{\infty} a^{2} f(a) \mathrm{d}a}, \qquad (21)$$

where $f(a)$ is the particle size distribution and $P(\sigma)$ is described by Eq. (19).

## 5. Conclusions

The experimental measurements of the small-angle patterns of particulate media show that the influence of multiple light scattering causes the broadening of the angular spectrum of the transmitted light and reduces the intensity of the Fraunghofer rings for monodispersed particles. One can see that Eqs. (15) and (16) describe the experimental data with a high accuracy. Thus they can be used as a theoretical basis for the laser diffraction spectroscopy of turbid media.

The function $\langle P(\sigma)\rangle$ in Eq. (21) can be retrieved from Eq. (10) by the inverse Fourier–Bessel transform. On the other hand, the Fourier–Bessel transform of the function $\langle P(\sigma)\rangle$ [see Eq. (12)] allows us to obtain the function $p(\theta)$ [see Eq. (1)] and reduce the inverse problem for a multiply light-scattering medium to the well-studied case of single scattering.

It is interesting to note that integral equation (1) can be solved analytically by use of the generalized Fourier transform.[14] Thus three successive integral transforms allow us to obtain the analytical solution for the particle size distribution from measurements of the diffused transmitted light in the multiple-scattering regime. Other possibilities for solving the inverse problem associated with Eq. (10) are discussed in Ref. 17.

A. A. Kokhanovsky is grateful to the Alexander von Humboldt Foundation (Germany) and the Engineering and Physical Sciences Research Council (United Kingdom) for support of this research. He thanks A. G. Borovoi and E. P. Zege for many fruitful discussions on the subject. Special thanks are ex-

tended to A. R. Jones for valuable comments and help.

## References

1. W. Witt and S. Röthele, "Laser diffraction—unlimited," Part. Part. Syst. Charact. **13,** 280–286 (1996).
2. K. S. Shifrin and G. Tonna, "Inverse problems related to light scattering in the atmosphere and ocean," Adv. Geophys. **34,** 175–252 (1993).
3. P. H. Kaye, K. Alexander-Buckley, E. Hirst, S. Saunders, J. M. Clark, "A real time monitoring system for airborne particle shape and size analysis," J. Geophys. Res. D **101,** 19215–19221 (1996).
4. 2600 Particle Sizer User Manual (Malvern Instruments, Malvern, UK, 1985).
5. S. M. Puckhaber and S. Röthele, "Laser diffraction: millenium-link for particle size analysis," Powder Handling Process. **11,** 91–95 (1999).
6. L. P. Bayvel, J. Knight, and G. Robertson, "Application of the Shifrin inversion to the Malvern particle sizer," in *Optical Particle Sizing*, G. Gouesbet and G. Grehan, eds. (Plenum, New York, 1988), pp. 311–319.
7. V. F. Belov, A. G. Borovoi, N. I. Vagin, and S. N. Volkov, "On small-angle method under single and multiple light scattering," Izv. Acad. Nauk SSSR Fiz. Atmos. Okeana **20,** 323–327 (1984).
8. N. I. Vagin and V. V. Veretennikov, "Optical diagnostics of disperse media under multiple scattering in small angle apptoximation," Izv. Acad. Nauk SSSR Fiz. Atmos. Okeana **25,** 723–731 (1989).
9. E. D. Hirleman, "Modelling of multiple scattering effects in Fraunhofer diffraction particle size analysis," Part. Part. Syst. Charact. **5,** 57–65 (1988).
10. E. D. Hirleman, "General solution to the inverse near-forward-scattering particle sizing problem in multiple-scattering environments: theory," Appl. Opt. **30,** 4832–4838 (1991).
11. H. Schnablegger and O. Glatter, "Sizing of colloidal particles with light scattering: corrections to beginning multiple scattering," Appl. Opt. **34,** 3489–3501 (1995).
12. L. S. Dolin, "About scattering of light beam in a layer of a turbid medium," Izv. Vyssh. Uchebn. Zaved. Radiofiz. (Sov. Radiophys.) **7,** 380–382 (1964).
13. E. P. Zege, A. P. Ivanov, and I. L. Katsev, *Image Transfer through a Scattering Medium* (Springer-Verlag, Berlin, 1991).
14. K. S. Shifrin, *Introduction to Ocean Optics* (Gidrometeoizdat, Leningrad, 1983).
15. E. P. Zege and A. A. Kokhanovsky, "Analytical solution to the optical transfer function of a scattering medium with large particles," Appl. Opt. **33,** 6547–6554 (1994).
16. A. A. Kokhanovsky, *Light Scattering Media Optics: Problems and Solutions* (Wiley-Praxis, Chichester, UK, 1999).
17. V. E. Zuev, V. V. Belov, and V. V. Veretennikov, *Linear Systems Theory in Optics of Disperse Media* (Siberian Brunch of the Russian Academy of Sciences, Tomsk, Russia, 1997).
18. K. S. Shifrin, *Scattering of Light in a Turbid Medium* (Gostekhteorizdat, Moscow, 1951) (English translation of NASA Tech. Trans. TT F-447, NASA, Washington, D.C., 1968).
19. H. C. van de Hulst, *Light Scattering by Small Particles* (Wiley, New York, 1957).